HHS Public Access

Author manuscript

Bone. Author manuscript; available in PMC 2019 November 01.

Published in final edited form as:

Bone. 2018 November ; 116: 135–143. doi:10.1016/j.bone.2018.07.020.

Calcium fluxes at the bone/plasma interface: acute effects of parathyroid hormone (PTH) and targeted deletion of PTH/PTH-related peptide (PTHrP) receptor in the osteocytes

Christopher Dedic[1], **Tin Shing Hung**[2], **Alan M. Shipley**[3], **Akira Maeda**[4,6], **Thomas Gardella**[4], **Andrew L. Miller**[2], **Paola Divieti Pajevic**[1], **Joseph G. Kunkel**[5], and **Alessandro Rubinacci**[7]

[1]Molecular and Cell Biology, Goldman School of Dental medicine, Boston University, Boston, MA, USA

[2]Division of Life Sciences and State Key Laboratory for Molecular Neuroscience, HKUST, Hong Kong, China

[3]Applicable Electronics, LLC, New Haven, CT, USA

[4]Endocrine Unit, Massachusetts General Hospital, Boston, USA

[5]Pickus Center for Biomedical Research, University of New England, Biddeford, ME, USA

[6]Chugai Pharmaceutical, San Raffaele Scientific Institute, Milano, Italy.

[7]Bone Metabolism Unit, San Raffaele Scientific Institute, Milano, Italy.

Abstract

Calcium ion concentration ($[Ca^{2+}]$) in the systemic extracellular fluid, ECF-$[Ca^{2+}]$, is maintained around a genetically predetermined set-point, which combines the operational level of the kidney/and bone/ECF interfaces. The ECF-$[Ca^{2+}]$ is maintained within a narrow oscillation range by the regulatory action of Parathyroid Hormone (PTH), Calcitonin, FGF-23, and $1,25(OH)_2D_3$. This model implies two correction mechanisms, i.e. tubular Ca^{2+} reabsorption and osteoclast Ca^{2+} resorption. Although their alterations have an effect on the ECF-$[Ca^{2+}]$ maintenance, they cannot fully account for rapid correction of the continuing perturbations of plasma $[Ca^{2+}]$, which occur daily in life. The existence of Ca^{2+} fluxes at quiescent bone surfaces fulfills the role of a short-term error correction mechanism in Ca^{2+} homeostasis.

To explore the hypothesis that PTH regulates the cell system responsible for the fast Ca^{2+} fluxes at the bone/ECF interface, we have performed direct real-time measurements of Ca^{2+} fluxes at the surface of *ex-vivo* metatarsal bones maintained in physiological conditions mimicking ECF, and exposed to PTH. To further characterize whether the PTH receptor on osteocytes is a critical component of the minute-to-minute ECF-$[Ca^{2+}]$ regulation, metatarsal bones from mice lacking the PTH receptor in these cells were tested *ex vivo* for rapid Ca^{2+} exchange. We performed direct

Address for correspondence: Alessandro Rubinacci, Bone Metabolism Unit, Scientific Institute San Raffaele, Via Olgettina 60, 20132 Milan, Italy, alessandro.rubinacci@hsr.it.

real-time measurements of Ca^{2+} fluxes and concentration gradients by a scanning ion-selective electrode technique (SIET). To validate *ex vivo* measurements, we also evaluated acute calcemic response to PTH *in vivo* in mice lacking PTH receptors in osteocytes vs littermate controls.

Our data demonstrated that Ca^{2+} fluxes at the bone-ECF interface in excised bones as well as acute calcemic response in the short-term were unaffected by PTH exposure and its signaling through its receptor in osteocytes. Rapid minute-to-minute regulation of the ECF-[Ca^{2+}] was found to be independent of PTH actions on osteocytes. Similarly, mice lacking PTH receptor in osteocytes, responded to PTH challenge with similar calcemic increases.

Keywords

Calcium Homeostasis; PTH; Osteocytes; Scanning ion-selective electrode technique (SIET)

INTRODUCTION

Calcium ion concentration ([Ca^{2+}]) of the extracellular (or plasma) fluid (ECF-[Ca^{2+}]) is held at a genetically predetermined set-point (1, 2), where ECF-[Ca^{2+}] is maintained within a narrow oscillation range by the regulatory action of parathyroid hormone (PTH), calcitonin (CT), $1,25(OH)_2D_3$ (3–5) and fibroblast growth factor-23 (FGF23) (6, 7) on the kidney- and on bone/plasma interfaces. This classical model of “reactive homeostasis” (8) implies two controllers, i.e. tubular Ca^{2+} reabsorption and osteoclast-mediated bone resorption. Although contributing to ECF-[Ca^{2+}] maintenance (9–11), they cannot be responsible for rapid and effective correction of the perturbations of plasma [Ca^{2+}] which occur in daily life (7, 12–15). Firstly, the amount of Ca^{2+} available in the distal nephron for error correction is minimal as approximately 98% of the filtered load is already reabsorbed (16), and the average daily flux due to distal nephron reabsorption is three to ten times lower than the rapid Ca^{2+} exchange at the bone/plasma interface (17). Second, the amount of bone resorbed by pre-existing osteoclasts under normal condition is insufficient to provide an adequate Ca^{2+} aliquot to adjust the short-term error to restore, minute-to-minute, normal ECF-[Ca^{2+}] (12, 18). Indeed, the rapid Ca^{2+} exchange at the bone/plasma interface is higher than the average daily flux due to bone turnover regardless of the degree of mineralization or turnover state (19). It is also worth considering that bisphosphonates cause significant decreases in bone resorption and they have no effect on PTH action to normalize plasma Ca^{2+} (20), and that autosomal dominant osteoporosis in adults is not accompanied by relevant alteration of ECF-[Ca^{2+}] (21).

Bone contains an exchangeable Ca^{2+} pool as a component of the extracellular fluid filling the lacuno-canalicular network (BECF) which encloses the osteocyte cell bodies and dendrites within the mineralized bone matrix (22). Since it has been recently estimated that BECF-volume is small, accounting for ~24 mL (23), the mineral-ion reservoir function of bone is mainly mediated by the structured hydrated layer, composed by loosely bound bivalent cations bound to the surface of apatite nanocrystals as well as to the organic phase (24, 25) that are instantly exchangeable with the plasma (26). By considering that the total surface area of the lacuno-canalicular system is ~$215m^2$ (23), the fast and reversible ion exchanges might be very efficient as a short-term buffer to sustain Ca^{2+} homeostasis and

skeletal integrity. Models proposed by Neuman (27), Talmage (15, 28), Bronner (17, 29) and Parfitt (13, 18) support the concept of a dynamic bone/plasma Ca^{2+} dis/equilibrium possibly modulated by the saturation level of hydroxyapatite solubility and/or access to Ca^{2+} binding sites. Novel mathematical models have also been developed to integrate this fast component in the slow-reacting Ca^{2+} homeostasis (30–32), but its hormonal regulation remains unsettled despite its importance in the overall plasma Ca^{2+} homeostasis. Experiments and models addressed to assess the contribution of PTH [see (13, 15, 18) for reviews] have suggested that the level of blood/bone equilibrium might vary with the level of PTH, but the direct experimental evidence for the PTH effect at the bone surface in eliciting a fast homeostatic response is lacking. As discussed by Parfitt (18), if and how PTH exert any action at this level “remains a mystery”.

Direct experimental evidences that bone plays a central role in the short-term error correction of plasma [Ca2+] without the contribution of bone remodeling were given by our group (33), which confirmed the Neuman’s observation (27): when a disequilibrium occurs between bone and plasma, ECF-[Ca2+] is corrected almost instantaneously. We performed direct real-time measurements of Ca2+ fluxes at the bone/plasma interface using a scanning ion-selective electrode technique (SIET), which allows a non-invasive measure of differences in specific ion concentration just outside a living membrane (34). The SIET measurements of the local Ca2+ concentration gradient (<10 μm spatial resolution) after exposing ex vivo metatarsal bones to the bathing solution, whose composition mimicked ECF, showed influxes of Ca^{2+} that reversed to effluxes when we depleted Ca^{2+} from ECF, mimicking a plasma demand. The reversal from influx to efflux and *vice versa* was immediate and fluxes were steady throughout the experimental time. Only the efflux was annulled within 10 minutes by the addition of Na-Cyanide, demonstrating its living-cell dependence.

We hypothesized that the cellular system able to rapidly fulfill the plasma Ca^{2+} homeostatic demand by sustaining an effective Ca^{2+} efflux from bone without activating remodeling might be the osteocyte-bone lining cell syncytium (OBLCS). Both interacting constituents of OBLCS, have receptors for PTH and can play a role in the short-term error correction mechanism by modulating the Ca^{2+} aliquots needed to correct ECF-[Ca^{2+}]. Osteocytes can modulate the availability of Ca^{2+} from the mineralized matrix without the need to activate an osteoclast-like function of matrix lysis (35) since they are ideally placed to establish a direct and extensive contact to a mineralized matrix (36, 37); can regulate virtually every phase of the mineralization process (36); can dissolve minerals through canaliculi by acidifying their microenvironment, and then transfer it to the bloodstream (38, 39); and can mobilize Ca^{2+} under sclerostin-exposure by up-regulating carbonic anhydrase 2, a major generator of H^+ (40).

In addition, it has been proposed that bone lining cells (BLCs), covering the quiescent surfaces of bone, might constitute a “bone membrane” (10, 41–48), acting as a partition system between BECF and ECF (48–51).

To explore the hypothesis that the cell system responsible for Ca^{2+} fluxes at the BECF-ECF interface is under PTH control, we have performed direct real-time measurements of Ca^{2+}

fluxes at the bone/plasma interface in metatarsal bones maintained *ex-vivo* under physiological conditions and exposed to PTH. Then, to further characterize whether the PTH/PTHrP receptor (PPR) located on osteocytes is a critical component of the minute-to-minute ECF-[Ca^{2+}] plasma Ca^{2+} regulation, metatarsal bones from mice lacking the PTH receptor on osteocytes (DMP1-Cre:PPRfl/fl) (52, 53) have been isolated and tested for rapid calcium exchange. Direct real-time measurements of Ca^{2+} fluxes and concentration gradients at the bone/plasma Ca^{2+} interface in isolated *ex-vivo* bone using SIET offered the unique opportunity to determine how Ca^{2+} gets into and out of bone almost instantaneously and what regulates its movement. To validate the *ex-vivo* SIET measurement, DMP1-Cre:PPRfl/fl mice were treated with PTH, and the acute changes in plasma Ca^{2+} were evaluated in comparison with their control littermates. We report here for the first time that acute treatment with PTH did not modify the instantaneous Ca^{2+} fluxes at the bone/plasma interface and that the receptor activation in osteocytes was not a critical component of the bone contribution to the short-term error correction mechanism(s) in plasma Ca^{2+} homeostasis.

This study addressed the characterization of a physiological function with a direct translational value. Deviation of plasma Ca^{2+} from set-point modulates osteoclastogenesis (54) and has profound effects on bone cell fate and activities, by means of the Ca^{2+} sensing receptor (CaSR) and independently of systemic calciotropic peptides (55). Moreover, plasma Ca^{2+} instability is critical in CKD-MBD (14), osteoporosis (15, 56), PTH related disorders and RANKL inhibition (30, 31) as well as cardiovascular diseases (57, 58).

MATERIALS AND METHODS

Metatarsal preparation

Incubation media were prepared as previously described (33). Living metatarsal bones were dissected in a medium containing physiological concentrations of the ions present in plasma, and defined $HCO3^{-}$-free ECF containing: $NaCl_2$ (96 mM/L), Na_2HPO_4 (1.35 mM/L), NaH_2PO4 (0.45 mM/L), KCl (4 mM/L), Ca-Lactate (1.5 mM/L), MgSO4 (0.7 mM/L), Na-Isethionate (30.85 mM/L), Glucose (28 mM/L), Mannitol (43.75 mM/L), Hepes (10 mM/L). Bicarbonate was excluded from the dissection medium to avoid physicochemical changes of the solution due to the CO_2 volatility and was replaced in the experimental solution to assure physiological conditions, as in the pioneering experiment (50). For SIET measurement (see below), the metatarsal bones were placed in a control medium containing physiological concentrations of bicarbonate by substituting 27 mM/L of Na-isethionate with 27 mM/L of $NaHCO_3$, and covered with a layer of mineral oil (Mineral Oil, Squib). As previously described (44), the unique design of the experimental chamber and the use of mineral oil was aimed at reducing to a reasonable minimum the exchange of CO_2 between the incubation medium and the ambient atmosphere. This experimental set-up was shown to be suitable for the study described here where the total elapsed time for the measurements obtained in bone incubated in a medium containing bicarbonate did not exceed 35 minutes. Furthermore, 10 mM HEPES buffer minimizes pH alterations.

All reagents were purchased from Sigma (St. Louis, MO). All experiments on living metatarsal bones were performed at a controlled temperature, 37°C. The pH was maintained

at 7.4 ± 0.1 at 37°C. Measured osmolality was systematically controlled and matched the theoretical value with 5% error. Human PTH(1–34) (MGH Peptide Core Facility) was dissolved in 0.1% trifluoroacetic acid (TFA), aliquoted, stored frozen at –80°C, and subsequently diluted to the appropriate concentration in vehicle) immediately before use.

Isolation of metatarsal bones was done as previously described (33, 42–44). Briefly, weanling mice, both littermate controls (C57BL/6 and PPRfl/fl) and study (DMP1-Cre:PPRfl/fl), between 19–21 days old were euthanized with Isoflurane (Piramal Healthcare, Cat#66794–017-25) followed by cervical dislocation.

The back limbs were amputated at the distal tibia epiphysis and immersed in the dissection medium to avoid pH changes during manipulations. The metatarsal bones (approximately 7 mm long and 1 mm thick) were carefully dissected to avoid damage to the bone surface. All manipulations were carried out on samples immersed in the dissection medium using a surgical microscope. After the metatarsal bone was freed of soft tissue ensheathments, the diaphysis was systematically cut by a surgical knife at 1/7 of the overall length. The distal 3/10 fragment (including the growth plate) was discarded, and the 7/10 proximal fragment was retained for the analysis. In this way the area of bone cortex exposed to the bathing fluid was kept constant, thus representing an advantage in terms of signal analysis with respect to the previous procedure of drilling a hole through the cortex (33) (Fig 1).

Mice

The use of animals for the metatarsal extraction and measurement was approved by the local (Marine Biological Laboratory, Woods Hole, MA) Institutional Animal Care and Use Committee.

DMP1-Cre:PPRfl/fl (or DMP1-PPR^{KO}) animals and littermate controls were generated by mating mice in which 10KbDMP1 promoter drives the expression of Cre-recombinase (10Kb DMP1-Cre, kindly provided by Dr. J. Feng) with mice in which the E1 exon of the PPR gene is flanked by lox-P sites (control, kindly provided by Dr. T. Kobayashi), as previously described (53). The genotypes of the mice were determined by PCR analysis of the genomic DNA extracted from tail biopsies. For the 10Kb Dmp1-Cre transgene, the forward Cre primer (5’-CGCGGTCTGGCAGTAAAAACTATC-3’) and the reverse Cre primer (5’-CCCACCGTCAGTACGTGAGATATC-3’) were used to generate a PCR product of approximately 400bp. For the floxed PPR allele, the P1 primer (5’-ATGAGGTCTGAGGTACATGGC TCTGA-3’) and the P2 primer (5’-CCTGCTGACCTCTCTGAAAGAATGT-3’) were used, which recognized the sequence spanning the 3’lox-P site, as previously reported (53). Wild-type and mutant alleles give ~ 210 bp and 290 bp products, respectively. The Institutional Animal Care and Use Committee, Subcommittee on Research Animal Care, at Massachusetts General Hospital approved all animal protocols for animal models generation.

Scanning ion-selective electrode technique (SIET)—basic principles

Key reviews reporting representative experiments have been recently published (34, 59) and the SIET basic principles have been outlined (60).

The SIET measures the free-ion concentration gradient of a specific ion (depending on the sensitivity of the selected tip-ionophore used, in our case Ca^{2+}) by means of repeatedly moving an ion-sensitive microelectrode (ISM) between two measurement points in the bulk media, one just outside the bone specimen and the other a fixed distance away (typically in the 10 μm range) using stepper motors controlled by software (ASET-LV4 Program, Science Wares, Inc. Falmouth, MA, USA) at programmed repetition rates slower than 1 Hz (typically 0.3 to 0.5 Hz range). A move-wait-measure progression scheme is employed. Specifics of the system applied have been described in detail (33). In short, the difference in voltage from the ISM between the two measurement points determines the flux magnitude as a function of the difference between the two measured Ca^{2+} concentrations. The ion flux was calculated using Fick's law of diffusion:

$$J = Cu\,(dc/dx)$$

where J is the ion flux in x direction, where C is the ion concentration in the solution; u is the ion mobility; and dc is the concentration difference over distance dx (see Fig. 1). The ISM potential in standard solutions containing different Ca^{2+} concentrations was used to construct a calibration curve to calculate the actual ion concentration. As the ISM moves in an ion gradient, near a source or sink of ion flux, the potential on the ISM varies in proportion to the size of the flux (J). A higher value at the position near to the bone surface indicates an outward ion flux (efflux).

Micrometer-tip size ion-selective electrode, ISM

Micrometer-tip size ISMs are extremely useful tools for measuring specific ion fluxes around embryos, organs, tissues and single cells. Ca^{2+}-specific ISM for bone measurement at 37°C have been previously described (33). Briefly, the ISM begins as a 1.5 mm diameter borosilicate glass capillary (TW150–4; World Precision Instruments Inc, Sarasota, FL, USA), pulled in two stages on a Flaming Brown Model P-97 electrode puller (Sutter Instruments, Novato, CA) to obtain a tip diameter ranging from 3 to 5 μm. The microelectrodes were then backfilled with 100 mM $CaCl_2$ electrolyte to a column length of ~1 cm, and front-loaded with a 30- to 40-μm-long column of liquid ion exchanger (LIX) (Fluka Chemie AG Ca^{2+} ionophore 1, cocktail A, Buchs, Switzerland). The ISM was then connected to an ion head-stage amplifier (Applicable Electronics LLC) via a short piece of silver chloride plated silver (Ag/AgCl) wire. This assembly acted as the measuring ISM. A new ISM was made for every experiment as required. The reference electrode was an Ag/AgCl half-cell (#MEH3S, World Precision Instruments, Inc., FL, USA), connected to the bone bathing (or calibration) solution by a PVC capillary tube filled with 3 M KCl and 0.5% agar. Before each experiment the ISM was tested against a series of Ca^{2+}-containing calibration solutions (i.e., containing 0.1 mM, 1.0 mM and 10.0 mM Ca Cl_2). ISMs with a deviation in their Nernst Slope of more than 3 mV from the theoretic value (i.e., between 27 and 33 mV) were discarded and a new ISM fabricated.

SIET experimental set-up and data acquisition

The experimental set-up was similar to the one previously described (33) with the exception of new software (ASET-LV4); improved digital imaging; and improvements to the 37°C

temperature control system. The metatarsal bone was held by drops of cyanoacrylate glue [Loctite® Super Glue, Westlake Ohio 44145] at the proximal extremity on a piece of a nylon washer fixed at the bottom of a standard 3.5-cm plastic Petri dish and the bone-shaft was held parallel to the bottom of the dish to allow for ISM scanning of the exposed bone cortex of the distal extremity minimizing the risk of ISM tip damage (Fig. 1). The dish was filled with the appropriate pre-warmed (37°C) medium (5.4 mL) and positioned on the viewing stage. The ISM was then immersed in the medium after which the medium surface was immediately covered with a thin layer of light, clear, pre-warmed (37°C) mineral oil. Contact between the oil layer and the ISM tip was avoided because the oil adversely affects the ionophore performance in the ISM tip. The oil layer also greatly reduces temperature-driven convection flow in the medium that causes instability in the Ca^{2+} gradient, and helps maintain pH by minimizing air-exchange at the surface of the solution. The oil layer also allows microscopic viewing of the specimen without any obstructions (see Fig. 1).

The environment inside the Faraday cage was maintained by a temperature controller (two quartz heater elements, OMEGA Part# OTF-192/240, one controlled by a variable transformer, the other controlled by a Temperature Control unit, OMEGA Model # CNI-3244). Temperature was controlled via a thermocouple probe placed beside the experimental dish connected to the heat control unit. A digital camera (Imaging Development Systems, Germany, Model # UI-1240SEuEYE, 1.3 Megapixel) was placed on an Optem Zoom 70 video zoom scope (magnification range: 5–45X, Thales-Optem, Fairport, NY, USA) then connected to a USB port on the DELL T-3500 PC. A National Instruments IMAQ Digital Interface was used to process the camera image and display it on an added PC monitor (PC had 2 monitors, one for program, one for image). Light was provided through a fiber-optic ringlite (Optem) connected to a light source (Dolan-Jenner, Model DJ-170). In this way, it was possible to run the experiment within the closed Faraday cage and visualize the motion of the ISM on an additional DELL flat screen monitor outside the Faraday cage, connected to the DELL PC. The cage was opened briefly for the addition of PTH (1 min) to the Petri dish containing metatarsals. A thin, clear vinyl curtain with a slit in the middle covered the access to the Faraday cage to minimize heat loss when the doors were open.

All SIET measurements were taken in the experimental medium. After stabilization of the readings at a fixed distance of 2 mm from the exposed bone cortex, here defined “at reference”, and after having mapped the spatial distribution of the Ca^{2+} fluxes, the ISM was located at the point of maximal flux over the exposed cortex, here defined “at bone” (see Fig. 1). The flux magnitude was first recorded for five minutes in the ECF and then 600μL of ECF containing PTH or vehicle (control) was added in the 5.4 mL of experimental ECF to give a final concentration of 100nMol of PTH in the final volume of 6 ml of ECF. The ISM was left at the same location before and after PTH addition for 20 minutes, then reported at the “reference” position for three minutes. Total elapsed time for the experiments was about 35 minutes. The same medium was left in the dish no longer than 30 min. This is the time-frame in which medium containing bicarbonate is known to be stable in this set-up from previous experiments (44). All movements were controlled via the ASET software. To assess any potential disturbance of the recordings due to PTH, additional experiments (n=3) were performed by adding PTH in absence of bone and no specific effects were observed.

Bone mineral structure analysis

To study the mineral content of the metatarsal bones excised from DMP1-PPR^{KO} animals and littermate controls, we applied the same electron microprobe analysis developed to study the mineral fine structure of American lobster cuticle, as previously described (61). Briefly, the liquid nitrogen frozen bone samples were embedded, after having been plunged in liquid-nitrogen-chilled acetone, in Epo-Thin Resin (Buehler), and finely polished to obtain a flat smooth surface.

The specimens were examined via a Cameca SX-50 Electron Microprobe (Madison, WI 53711, USA) to provide electron probe microanalysis (EPMA) for a chosen list of ions PO^{4-}, Mg^{2+}, Ca^{2+}, Ba^{2+}, Mn^{2+}, K^{+}, and Na^{+}. The SX-50 allows for a set of ions, measured simultaneously at each location. Data from the EPMA instruments were subsequently exported and analyzed as reported.

Acute PTH injection in vivo

For *in vivo* acute PTH administration 8–10 weeks old male (n=4 in each group) mice were injected with vehicle (10 mM citric acid/150 mM NaCl/0.05% Tween-80, pH 5.0) or vehicle containing human PTH (1–34) at doses of 50 nmol/kg or a mutated long-acting PTH analog (LA-PTH) at 10 nmol/kg (62) after a 2 weeks of wash-out following the first experiment. Blood was collected from the tail vein and analyzed directly for Ca^{2+} using a Siemens RapidLab 348 Ca2+/pH analyzer. Plasma cAMP was measured by radioimmunoassay (RIA) using a commercial cAMP assay kit (New England Nuclear Corp., Boston, MA). Data were processed using Excel 2008 (Microsoft Corp.) and Prism 5.0 (GraphPad Software Inc.). Statistical analyses used the Student-t test (two-tailed, unequal variances), with significance inferred from P values of 0.05 or less.

Cyclic AMP measurement

Metatarsal were isolated from 19–21 days old WT animals, as described above. Each metatarsal was then placed in ice-cold cAMP-assay buffer (Dulbecco Modified Essential Medium containing 10 mM HEPES, 0.1% heat-inactivated BSA and 1 mM isobutylmethylxantine) or in modified cAMP-assay buffer. Bone pieces were then incubated in cAMP-assay buffer with the appropriate treatment at 37°C for 15 min. Three to five metatarsal were incubated with vehicle alone (assay buffer), 100 nM human PTH (1–34) or 0.1 μM forskolin. At the end of the incubation, the reaction was terminated by quickly removing the bones and placing them in 0.3 ml of cold 90% 2-propanol in 0.5 M HCl. Bones were then incubated for 16–18 h at 4°C. Propanol extraction was repeated, and the combined extracts were evaporated by vacuum centrifugation. The dried extracts were dissolved in acetate buffer (50 mM Na acetate/0.05% Na azide, pH 6.2) for measurement of cAMP by a specific in-house RIA, as previously described (53). cAMP RIA was done by the Center for Skeletal Research at Mass General Hospital, Boston, MA. Bones were washed twice with 0.5 ml acetone and once with 0.5 mL ether and were air-dried and weighed. The results were normalized for the bone weight, and the data were expressed as picomole of cAMP produced per mg of dry bone. Each experiment was done at least three times.

Data analysis

Data from the ion probe were recorded by the ASET software (Science Wares, Falmouth, MA) into comma-separated value files (CMV) with a time-base, location, and a mV measure of Ca^{2+} titer and a second mV reading 10 μm away from which a flux calculation is made in that direction (33). The two measures of Ca^{2+} activity, concentration, directional flux, and place were recorded for measured times under applied treatment regimes. Plots of the continuous recording of log of concentration and the flux of Ca^{2+} were amended for the times of drug-addition and opening of the Faraday cage. The resulting data was smoothed using the LOESS function of R-Core team [R Foundation for Statistical Computing, Vienna, Austria. 2016]. The significance of the treatments was judged from comparisons of at least three replicates of each treatment-response curve considering the standard errors of departure from the fitted curves. Atomic abundance data from the SX-50 EPMA analysis was measured versus μm displacement of the electron beam along the linear scan track. A LOESS smoothing of the X-ray atomic abundance estimates are provided with 95% Confidence Interval (CI) standard error of the mean departure from the curve is indicated as a vertical bar. Data from the EPMA instrument were exported and analyzed by multivariate analysis of dispersion and test for additional information according to Rao (63).

RESULTS

Acute PTH does not affect Ca^{2+} fluxes in metatarsal bone

Initial studies were performed to investigate whether PTH was able to acutely induce changes in Ca^{2+} influx in *ex vivo* metatarsal bones. As previously reported, in conditions in which the bones were bathed in medium having the same ionic composition as plasma, there was a net influx of Ca^{2+} entering the bone at the cut site. The maximal Ca^{2+} influx was present at the edge of the metatarsal bone and the flux decreased when the probe was moved away from the bone surface. We investigated whether the maximal Ca^{2+} influx was affected by PTH. The hormone (100 nM human PTH(1–34) was added to the metatarsal medium and the Ca^{2+} fluxes at the bone site were recorder for 5 consecutive minutes. As shown in the boxplot in Fig. 2A, there were no significant changes in Ca^{2+} fluxes at the bone site when the hormone was added (marked as PTH0), suggesting that the minute-to-minute Ca^{2+} current at the bone surface is independent of PTH action. The boxplot graph, showing the mean $[Ca^{2+}]$ at the beginning of the experiment, at reference (R1) and near the surface of the bone (B) and at different times upon administration of PTH (PTH1–3), indicates that there are no changes in the ECF $[Ca^{2+}]$ (Fig. 2A). We then analyzed the Ca^{2+} fluxes in metatarsal bones of animals lacking PPR expression in osteocyte, and exposed to PTH treatment. As shown in Fig. 2B, Ca^{2+}fluxes from *ex-vivo* metatarsal bones of DMP1-Cre:PPRfl/fl animals were similar to control littermates (PPR fl/fl), and the addition of PTH elicited no significant effect. The boxplot shows no changes in ECF $[Ca^{2+}]$ after PTH. As shown in Fig. 2C, the comparison of Ca^{2+} slopes soon after adding PTH demonstrated no significant difference between PPRfl/fl controls (WT) and KO bones. Taken together these data demonstrate that *ex vivo* metatarsal bones are capable of maintaining Ca^{2+} fluxes independently of PTH action, and that the hormone is not implicated in the minute-to-minute regulation of ECF-$[Ca^{2+}]$. To exclude the possibility that the lack of hormonal effect was related to the SIET experimental conditions, we performed an experiment in which cAMP accumulation in

response to PTH treatment was done in *ex vivo* metatarsal bone maintained under identical SIET conditions or in standard cAMP buffer (both containing phosphodiesterase inhibitors). As expected, there was a significant increase in cAMP upon PTH or forskolin treatment in bones cultured in both conditions, demonstrating that metatarsal bones do retain PTH-responsiveness (Fig. 3).

PTH receptor in osteocytes is not required for acute calcemic responses

It is well known that a single injection of PTH(1–34) into animals and humans results in an acute rise in blood [Ca^{2+}] and decrease in blood phosphate concentrations. Three organs participate in supplying Ca^{2+} to the blood: (i) The small intestine through the absorption of Ca^{2+} from the diet (vitamin-D dependent); (ii) The kidney through tubular reabsorption of Ca^{2+}; and (iii) The skeleton with the release of Ca^{2+} from bone. PTH acts directly, or indirectly, on these target organs but the mechanism by which the hormone rapidly (within hours) increases blood [Ca^{2+}] is not completely understood. One hypothesis put forward is that PTH can acutely release Ca^{2+} from the mineralized matrix surrounding the osteocytic lacuno-canalicular network. Since the data generated using the SIET and *ex vivo* metatarsal bones revealed no effect of either PTH administration or PPR ablation in osteocytes in regulating Ca^{2+} fluxes, we performed acute PTH injection in male DMP1-Cre:PPRfl/fl as well as PPRfl/fl littermate controls, in order to assess the role of PPR in osteocytes with regards to acute calcemic responses. Fig. 4A shows that in animals lacking PPR expression in osteocytes, PTH can elicit a full calcemic response, as demonstrated by a significant increase in Ca^{2+} after 1 and 2 hr of hormone administration. Serum [Ca^{2+}] returned to basal levels after 4 hours. DMP1-Cre:PPRfl/fl mice display full calcemic response to acute PTH administration, demonstrating that osteocytes do not participate in a PTH acute calcemic response, and that other bone cells, probably BLCs or osteoclasts, or other organs, might be driving the acute calcemic response. Lastly, we evaluated whether difference in acute calcemic responses between DMP1-Cre:PPRfl/fl and littermate controls could be elicited by injection with a long-acting mutated PTH (M-PTH 1–28). This peptide has been shown to have higher affinity for the R^0 PPR conformation, and to have, both *in vitro* and *in vivo*, a prolonged activity (62). Indeed, calcemic responses to PTH and M-PTH(1–28) - a long acting PTH analog - were similar in both DMP1-Cre:PPRfl/fl and control mice. Serum cAMP concentration, detected 15 minutes after PTH or M-PTH administration, was also identical between KO and control animals. These data support the proposition that PTH induces acute, transient, calcemic responses that are independent of its effect on osteocytes.

Lack of PTH receptor in osteocytes alters bone mineral composition

To further study the role of PPR in osteocytes in controlling mineral homeostasis, we analyzed the mineral composition of metatarsals from DMP1-Cre:PPRfl/fl and littermate controls. We did not find any significant difference between controls bones (n=3) in their composition of calcium, phosphorus, magnesium, sodium, potassium, strontium, barium, manganese composition based on EPMA ($P>0.999$). Conversely, we found a very highly significant difference between the atomic composition of DMP1-Cre:PPRfl/fl bone vs the littermate controls as a whole ($P<0.0001$). The greatest difference between DMP1-Cre:PPRfl/fl and littermate controls was contributed by strontium, barium and manganese as

indicated by their ratio of change, plotted in Fig 5. There was no significant additional contribution by magnesium (P>0.903) and potassium (P>0.837).

As shown in Fig. 5, in the absence of PPR, the level of Sr^{2+} was more than 3-fold higher in bone from KO mouse compared to controls. Interestingly, both Ca^{2+} and PO^{4-} levels were unaffected. This data indicates that in the absence of PTH receptor signaling on osteocytes, there is shift in the relative content of divalent cations and, in particular, a relative accumulation of Sr^{2+}.

DISCUSSION

Our study demonstrates that the immediately exchangeable Ca^{2+} pool available at the bone/plasma interface to contribute to plasma Ca^{2+} homeostasis is independent of the effects of PTH. *Via* the unique opportunity offered by SIET to obtain direct real-time measurements of Ca^{2+} fluxes and concentration gradients at the bone/plasma Ca^{2+} interface (34, 57, 58, 60), and by applying the previously validated method of *ex vivo* metatarsal bones in physiological conditions (33), we have now been able to provide the first direct demonstration that the immediately exchangeable Ca^{2+} fluxes at the bone/plasma interface are independent of PTH and its signaling in osteocytes. Indeed, acute PTH treatment was unable to affect Ca^{2+} fluxes in either DMP1-Cre:PPRfl/fl and controls metatarsal explants. Thus, our results noticeably challenged the general assumption that PTH is the critical regulatory factor, acting on bone surfaces to maintain stable plasma Ca^{2+} concentration on a rapid minute-to-minute basis.

The experiments described here were performed under a normal Ca^{2+} concentration in the external medium. This was done with the purposes to obtain a bone response in a physiological condition, to assure optimal probe sensitivity and stability, and to detect potential transient influx of Ca^{2+} into bone after PTH addition, as suggested by some early study with $^{45}Ca^{2+}$ (64). SIET is not exposed to bias as is radio-labeling Ca^{2+} - that remains sensitive to $^{40}Ca^{2+}/^{45}Ca^{2+}$ equilibration phenomena - and gives a direct real-time measurement of the net Ca^{2+} flux and $[Ca^{2+}]$ gradient at the extracellular level. The absence of a significant change of a SIET-detected Ca^{2+} flux at the bone/medium interface after PTH addition, rules out any specific action of the hormone on Ca^{2+} handling at the bone surface in the short-term. It is highly unlikely that we have missed a fast Ca^{2+} transient during the two minutes when SIET recording was interrupted due to the time needed for PTH addition and stabilization of the SIET signal, since any PTH-activated Ca^{2+} entry into the cytosol would have significantly affected the $[Ca^{2+}]$ at the bone surface in the very short term after PTH exposure. Under identical experimental conditions, the SIET was able to detect a fast Ca^{2+} efflux transient from the cytosol after cell poisoning (33).

In addition, any potential bias due to the specific model used (i.e *ex vivo* metatarsal bones) was ruled out because PTH treatment was found to be effective in eliciting an acute significant rise of cAMP concentration in excised metatarsal bones of weanling mice, placed in identical experimental conditions, therefore validating our experimental set-up, as shown in Fig. 3.

The present study has also shown that the Ca^{2+} fluxes at the bone/medium interface were unaffected in the short-term by specifically ablating the PTH/PTHrp receptor in osteocytes. Contrary to the generally acknowledged assumption that PTH/PTHrp receptor activation might have an effect on Ca^{2+} homeostasis through the reversible enlargement of the osteocyte lacunae and demineralization of the surrounding matrix under high Ca^{2+} demand (38, 39, 65), our study raises the hypothesis that minute-to-minute maintenance of Ca^{2+} equilibrium at the bone surfaces does not require any rapid action of PTH on the osteocytes. A further validation of the SIET results derives from our *in vivo* observation that acute injections of PTH in DMP1-Cre:PPRfl/fl mice elicits a calcemic response that is indistinguishable from control mice (PPRfl/fl littermates), thus confirming earlier reports (62). We can therefore suggest that PTH receptor signaling in osteocytes (or DMP1-positive cells) is not required for the acute calcemic effect of the hormone. Similarly, to the *ex vivo* experiment, the *in vivo* one was also confirmed by the contemporary measurement of serum cAMP which was found to be significantly increased in both DMP1-Cre:PPRfl/fl and control animals upon acute PTH administration.

Our study challenges earlier reports that have hypothesized that bone-mediated minute-to-minute regulation of plasma Ca^{2+} by PTH are due to Ca^{2+} transport from bone without osteolysis (66). When embryonic chick tibiae were exposed to PTH, a mechanism was envisaged for selectively moving Ca^{2+} out of bone, and maintaining Ca^{2+} level in the bone fluid lower than that in the general extracellular fluid (67). However, earlier studies were inconclusive, nor do they identify the source of Ca^{2+} (15, 28). Furthermore, the role of PTH in bone/plasma rapid Ca^{2+} equilibrium remained conjectural (13,18).

Recently, the concept that PTH signaling in bone is essential for Ca^{2+} homeostasis has been re-examined and a critical role for the PTHR-1 in regulating acute responses in target tissues has been reported (62). PTH induces indeed a calcemic response that is significant at 1 to 2 h post injection (62). However, the study outlined the importance of additional elements, as ambient Pi, of the overall homeostatic regulation of calcium by PTH, thus leaving the target cells in bone, beyond osteoclasts, undetermined. In order to selectively evaluate the role of osteocytes in plasma Ca^{2+} homeostasis, PTH/PTHrp receptor was specifically ablated in osteocytes and the plasma [$Ca2^{+}$] was found, respectively, to be reduced or not maintained in the DMP1-Cre:PPRfl/fl mice compared to littermate controls when subjected to a low Ca^{2+} diet (52). Conversely, in our study basal plasma [Ca^{2+}] did not differ between KO mice and controls when maintained on a regular diet (Fig 4A), thus in agreement with previous report (53). This difference can be reconciled by considering that the low plasma [Ca^{2+}] was detected only in DMP1-Cre:PPRfl/fl mice undergone to the challenge of a 2 weeks low Ca^{2+} diet. It is therefore conceivable that under a long-term dietary Ca^{2+} insufficiency, the role of the osteocytic PTH/PTHrp receptor can be highlighted as one element of the long-term error correction mechanisms in plasma [Ca^{2+}] homeostasis. Perilacunar osteocytes remodeling (68), and synergic osteoclastic activity through the RANK/RANKL pathway (69), which are expected to be reduced due to the ablation of PTH/PTHrp receptor, might require a time longer that the fast and reversible fluxes of Ca^{2+} at the bone/plasma interface following a physiological demand, as directly measured *ex vivo* by us in a previous study (33), and confirmed here. Both phenomena, i.e., perilacunar osteocyte remodeling as well as osteoclast resorption, require the reversible activation, in osteocytes as well as in osteoclasts,

of genes typically associated with bone resorption (70), and are induced under the physiological condition of a long-term high Ca^{2+} demand, such as during lactation (36, 65) and/or a low Ca^{2+} diet (52).

Our new study also challenge the recent observations that osteocytes can remove minerals from bone through acidification of their surrounding bone fluid and their perilacunar matrix under PTH infusion, as assessed with synchrotron X-ray tomographic microscopy (39), as well as in response to PTHrP exposure *in vitro*, and in lactating mice *in vivo* (38). These observations have raised the possibility that Ca^{2+} can be released to the bloodstream faster than expected since PPR activation can lower the microenvironment pH through a PTHrP-dependent stimulation of the ATP6V0D2, an essential component of vacuolar ATPase (V-ATPase), and subsequent H^+ generation in primary osteocytes (38). At present, however, the synchrotron X-ray tomographic microscopy does not allow *in vivo* time-course analyses (39), nor is it known the time required to achieve an efficient acidification of the mineralized matrix under PTH stimulation *via* V-ATPase in osteocytes (38). Thus, the relative contribution of PPR activation in osteocytes on the instantaneous and reversible Ca^{2+} fluxes *in/ex vivo via* acidification of the perilacunar matrix, remains unproven. One hypothesis might imply the contribution of “coastal crystals”, i.e., Ca^{2+} ions linked to a glycoprotein template and distributed on the surface of the osteocytic lacunae (71, 72). These crystals might be dissolved to fulfill minute-by-minute Ca^{2+} demands without the need of enlarge the osteocytcic lacuna. SIET could be applied to solve this question since it can provide a contemporary assessment of H^+ and Ca^{2+} fluxes at the bone/plasma interface in real-time (60, 61).

Of course, our study does not rule out the regulatory role of PPR under a prolonged calcemic challenge allowing the remodeling of the lacunae and/or the acidification of the mineral surface. Our finding that, in the absence of PPR signaling on osteocytes, there is a shift in the relative content of divalent cations in favor of strontium ions (Sr^{2+}) indicates an altered incorporation of foreign ions into the growing apatite domain of DMP1-Cre:PPRfl/fl animals. Sr^{2+} has chemical properties, hydrated radius and interactions similar to those of Ca^{2+}. It belongs to the category of foreign ions that are incorporated during the maturation of the apatite crystals, and it is no longer available for reverse exchange reactions (26). This suggests that the impaired function of PPR in osteocytes might have a long-term impact on the maturation of the apatite.

Our present demonstration that fast and reversible Ca^{2+} fluxes at the bone/plasma interface in the short-term are independent of PTH and its signaling in osteocytes, is in agreement with the *in vivo* observations that PTH is not essential for the rapid minute-to-minute regulation of plasma [Ca^{2+}]. In all these studies, the rapid recovery of plasma [Ca^{2+}] was examined after EGTA-related induction of hypocalcemia in parathyroidectomized rats, and rats treated with PTH (73). Given the stability of the Ca^{2+}-EGTA complex and the rapid increase in plasma [Ca^{2+}] after the brief induction of hypocalcemia in PTH depleted animals (74), the overall conclusion of these studies, as stated by the authors, was that PTH is not a prerequisite for the rapid correction of ECF-[Ca^{2+}], although they later observed that the recovery is influenced by the presence of what they described as a “kidney-bone axis” of minute-by-minute regulation of ECF-[Ca^{2+}] (7).

The present study is also in agreement with the observation that chronic inhibition of the Ca^{2+}-sensing receptor (CaSR) in thyro-parathyroidectomized rats selectively increases renal tubular ECF-[Ca^{2+}] absorption and blood [Ca^{2+}] independently of PTH and without altering intestinal Ca^{2+} absorption (75). The demonstration that the CaSR is a direct, PTH-independent determinant of blood [Ca^{2+}] (76) suggests that the CaSR - beyond being a component of the Ca^{2+}/PTH axis and a regulator of tubular Ca^{2+} reabsorption - might be essential in Ca^{2+} homeostasis for its potential role at the bone/plasma interface where it might regulate minute-to-minute Ca^{2+} fluxes as it does in the thick ascending limb of the loop of Henle. It has been indeed demonstrated that the recovery phase ECF-[Ca^{2+}] in thyro-parathyroidectomized rats was significantly impaired in rats treated with the CaSR activators, R-568 and gentamycin (77). It is worth noting that the CaSR modulates renal tubular Ca^{2+} transport via the permeability of the paracellular pathway to Ca^{2+} (75). It might be also involved at the bone/plasma interface as it is at the tubular/plasma interface. Furthermore, the CaSR might modulate paracellular Ca^{2+} transport trough the bone lining cells covering the quiescent surfaces, as well as along electrochemical and chemical gradients that are generated by a complex multi-ionic pump–leak systems (10, 42–44, 48). The existence of a “functional” epithelial-like bone membrane operating in Ca^{2+} homeostasis was foreseen by pioneering experiments based upon radioactive Ca^{2+} distribution in bone (78). Recently, this view is sustained by the observation that claudins (tight junction membrane proteins) have been reported to regulate and restrict paracellular ion transport at the bone/plasma interface according to the metabolic demand (79, 80). It has been suggested that sufficient mineral components can be supplied by bone lining cells that might change the permeability of the interface between the lacunar-canalicular porosity and the collagen-hydroxyapatite porosity (22, 56) and/or control the access to organic and inorganic Ca^{2+} binding sites (15, 41). Further studies should be undertaken to investigate possible CaSR-mediated modulation of paracellular Ca^{2+} transport through the bone lining cells, and thus regulating the permeability of the lacunar-canalicular/collagen-hydroxyapatite porosity interface. This phenomenon is worth consideration as potential mechanism underlying the minute-to-minute regulation of plasma Ca^{2+} homeostasis.

One limitation of this study is related to the lack of a positive control. However, at present, an endogenous regulator (or regulators) of instantaneous calcium fluxes at the bone-plasma interface remain unknown.

In conclusion, it can be argued that the fastest response in the continuous temporal hierarchy of events addressing a disruption in plasma Ca^{2+} homeostasis, is independent of PTH and its associated signaling through its receptor in osteocytes.

ACKNOWLEDGMENTS

This project was made possible by equipment and support provided by Applicable Electronics, LLC., New Haven, CT, USA. This work was supported by the National Institutes of Health grant DK079161 awarded to PDP; NIH DK011794 for TJG; as well as the Hong Kong JUSTL program grants CF06/07.SC04 and GMGS06/07.SC01 (that supported the rental of a laboratory at the MBL, Woods Hole, MA, during the summers of 2013, 2014, and 2015), the Hong Kong Research Grants Council General Research Fund grants 16101714 and 16100115, the ANR/RGC joint research fund grant A-HKUST601/13, and the Hong Kong Innovation and Technology Commission grant ITCPD/17-9, awarded to ALM. The Center for Skeletal Research Core (NIH P30 AR066261) conducted radioimmunoassay for cAMP. AM is an appointee of MGH and employee of Chugai Pharmaceutical Co., Ltd.

REFERENCES

1. Kurokawa K The kidney and calcium homeostasis. Kidney Int Suppl. 1994;44(S97–105). [PubMed: 8127042]
2. Kurokawa K How is plasma calcium held constant? Milieu interieur of calcium. Kidney Int. 1996;49(6):1760–4. [PubMed: 8743492]
3. Lieben L, and Carmeliet G. Vitamin D signaling in osteocytes: effects on bone and mineral homeostasis. Bone. 2013;54(2):237–43. [PubMed: 23072922]
4. Lieben L, and Carmeliet G. The delicate balance between vitamin D, calcium and bone homeostasis: lessons learned from intestinal- and osteocyte-specific VDR null mice. J Steroid Biochem Mol Biol. 2013;136(102–6). [PubMed: 23022574]
5. Mundy GR, and Guise TA. Hormonal control of calcium homeostasis. Clin Chem. 1999;45(8 Pt 2): 1347–52. [PubMed: 10430817]
6. Andrukhova O, Smorodchenko A, Egerbacher M, Streicher C, Zeitz U, Goetz R, Shalhoub V, Mohammadi M, Pohl EE, Lanske B, et al. FGF23 promotes renal calcium reabsorption through the TRPV5 channel. EMBO J. 2014;33(3):229–46. [PubMed: 24434184]
7. Nordholm A, Mace ML, Gravesen E, Olgaard K, and Lewin E. A potential kidney-bone axis involved in the rapid minute-to-minute regulation of plasma Ca2+. BMC Nephrol. 2015;16(29.
8. Moore-Ede MC. Physiology of the circadian timing system: predictive versus reactive homeostasis. Am J Physiol. 1986;250(5 Pt 2):R737–52. [PubMed: 3706563]
9. Bushinsky DA. Contribution of intestine, bone, kidney, and dialysis to extracellular fluid calcium content. Clin J Am Soc Nephrol. 2010;5 Suppl 1(S12–22). [PubMed: 20089498]
10. Bushinsky DA, Chabala JM, and Levi-Setti R. Ion microprobe analysis of mouse calvariae in vitro: evidence for a “bone membrane”. Am J Physiol. 1989;256(1 Pt 1):E152–8. [PubMed: 2912140]
11. Heaney RP. How does bone support calcium homeostasis? Bone. 2003;33(3):264–8. [PubMed: 13678766]
12. Bronner FExtracellular and intracellular regulation of calcium homeostasis. ScientificWorldJournal. 2001;1(919–25). [PubMed: 12805727]
13. Parfitt AM. Large calcium fluxes that are not related to remodeling exist. Bone. 2003;33(3):269. [PubMed: 14562830]
14. Pirklbauer M, and Mayer G. The exchangeable calcium pool: physiology and pathophysiology in chronic kidney disease. Nephrol Dial Transplant. 2011;26(8):2438–44. [PubMed: 21551087]
15. Talmage RV, and Mobley HT. The concentration of free calcium in plasma is set by the extracellular action of noncollagenous proteins and hydroxyapatite. Gen Comp Endocrinol. 2009;162(3):245–50. [PubMed: 19361508]
16. Hoenderop JG, Nilius B, and Bindels RJ. Molecular mechanism of active Ca2+ reabsorption in the distal nephron. Annu Rev Physiol. 2002;64(529–49). [PubMed: 11826278]
17. Bronner F, and Stein WD. Calcium homeostasis--an old problem revisited. J Nutr. 1995;125(7 Suppl):1987S–95S. [PubMed: 7602381]
18. Parfitt AM. Misconceptions (3): calcium leaves bone only by resorption and enters only by formation. Bone. 2003;33(3):259–63. [PubMed: 13678765]
19. Reeve J The turnover time of calcium in the exchangeable pools of bone in man and the long-term effect of a parathyroid hormone fragment. Clin Endocrinol (Oxf). 1978;8(6):445–55. [PubMed: 668151]
20. Jara A, Lee E, Stauber D, Moatamed F, Felsenfeld AJ, and Kleeman CR. Phosphate depletion in the rat: effect of bisphosphonates and the calcemic response to PTH. Kidney Int. 1999;55(4):1434–43. [PubMed: 10201008]
21. Bollerslev J Autosomal dominant osteopetrosis: bone metabolism and epidemiological, clinical, and hormonal aspects. Endocr Rev. 1989;10(1):45–67. [PubMed: 2666111]
22. Cardoso L, Fritton SP, Gailani G, Benalla M, and Cowin SC. Advances in assessment of bone porosity, permeability and interstitial fluid flow. J Biomech. 2013;46(2):253–65. [PubMed: 23174418]

23. Buenzli PR, and Sims NA. Quantifying the osteocyte network in the human skeleton. Bone. 2015;75(144–50). [PubMed: 25708054]
24. Wehrli FW, and Fernandez-Seara MA. Nuclear magnetic resonance studies of bone water. Ann Biomed Eng. 2005;33(1):79–86. [PubMed: 15709708]
25. Wilson EE, Awonusi A, Morris MD, Kohn DH, Tecklenburg MM, and Beck LW. Three structural roles for water in bone observed by solid-state NMR. Biophys J. 2006;90(10):3722–31. [PubMed: 16500963]
26. Rey C, and Combes C eds. Physical chemistry of biological apatites. Elsevier Ltd; 2016.
27. Neuman WF, Neuman MW, Diamond AG, Menanteau J, and Gibbons WS. Blood:bone disequilibrium. VI. Studies of the solubility characteristics of brushite: apatite mixtures and their stabilization by noncollagenous proteins of bone. Calcif Tissue Int. 1982;34(2):149–57. [PubMed: 6805920]
28. Talmage RV, Lester GE, and Hirsch PF. Parathyroid hormone and plasma calcium control: an editorial. J Musculoskelet Neuronal Interact. 2000;1(2):121–6. [PubMed: 15758504]
29. Bronner F, and Stein WD. Modulation of bone calcium-binding sites regulates plasma calcium: an hypothesis. Calcif Tissue Int. 1992;50(6):483–9. [PubMed: 1525701]
30. Granjon D, Bonny O, and Edwards A. A model of calcium homeostasis in the rat. Am J Physiol Renal Physiol. 2016;311(5):F1047–F62. [PubMed: 27358053]
31. Peterson MC, and Riggs MM. A physiologically based mathematical model of integrated calcium homeostasis and bone remodeling. Bone. 2010;46(1):49–63. [PubMed: 19732857]
32. Granjon D, Bonny O, and Edwards A. Coupling between phosphate and calcium homeostasis: a mathematical model. Am J Physiol Renal Physiol. 2017;313(6):F1181–F99. [PubMed: 28747359]
33. Marenzana M, Shipley AM, Squitiero P, Kunkel JG, and Rubinacci A. Bone as an ion exchange organ: evidence for instantaneous cell-dependent calcium efflux from bone not due to resorption. Bone. 2005;37(4):545–54. [PubMed: 16046204]
34. Reid B, and Zhao M. Ion-selective self-referencing probes for measuring specific ion flux. Commun Integr Biol. 2011;4(5):524–7. [PubMed: 22046453]
35. Cullinane DM. The role of osteocytes in bone regulation: mineral homeostasis versus mechanoreception. J Musculoskelet Neuronal Interact. 2002;2(3):242–4. [PubMed: 15758444]
36. Atkins GJ, and Findlay DM. Osteocyte regulation of bone mineral: a little give and take. Osteoporos Int. 2012;23(8):2067–79. [PubMed: 22302104]
37. Divieti Pajevic P Recent progress in osteocyte research. Endocrinol Metab (Seoul). 2013;28(4): 255–61. [PubMed: 24396689]
38. Jahn K, Kelkar S, Zhao H, Xie Y, Tiede-Lewis LM, Dusevich V, Dallas SL, and Bonewald LF. Osteocytes Acidify Their Microenvironment in Response to PTHrP In Vitro and in Lactating Mice In Vivo. J Bone Miner Res. 2017;32(8):1761–72. [PubMed: 28470757]
39. Nango N, Kubota S, Hasegawa T, Yashiro W, Momose A, and Matsuo K. Osteocyte-directed bone demineralization along canaliculi. Bone. 2016;84(279–88). [PubMed: 26709236]
40. Kogawa M, Wijenayaka AR, Ormsby RT, Thomas GP, Anderson PH, Bonewald LF, Findlay DM, and Atkins GJ. Sclerostin regulates release of bone mineral by osteocytes by induction of carbonic anhydrase 2. J Bone Miner Res. 2013;28(12):2436–48. [PubMed: 23737439]
41. Parfitt AM. Plasma calcium control at quiescent bone surfaces: a new approach to the homeostatic function of bone lining cells. Bone. 1989;10(2):87–8. [PubMed: 2765314]
42. Rubinacci A, Benelli FD, Borgo E, and Villa I. Bone as an ion exchange system: evidence for a pump-leak mechanism devoted to the maintenance of high bone K(+). Am J Physiol Endocrinol Metab. 2000;278(1):E15–24. [PubMed: 10644532]
43. Rubinacci A, Covini M, Bisogni C, Villa I, Galli M, Palumbo C, Ferretti M, Muglia MA, and Marotti G. Bone as an ion exchange system: evidence for a link between mechanotransduction and metabolic needs. Am J Physiol Endocrinol Metab. 2002;282(4):E851–64. [PubMed: 11882505]
44. RubinaccA, De PontA, ShipleA, SamajM, Karplus E, and Jaffe LF. Bicarbonate dependence of ion current in damaged bone. Calcif Tissue Int. 1996;58(6):423–8. [PubMed: 8661484]

45. Rubinacci A, Villa I, Dondi Benelli F, Borgo E, Ferretti M, Palumbo C, and Marotti G. Osteocyte-bone lining cell system at the origin of steady ionic current in damaged amphibian bone. Calcif Tissue Int. 1998;63(4):331–9. [PubMed: 9744993]
46. Scarpace PJ, and Neuman WF. The blood: bone disequilibrium. I. The active accumulation of K+ into the bone extracellular fluid. Calcif Tissue Res. 19762):137–49.
47. Soares AM, Arana-Chavez VE, Reid AR, and Katchburian E. Lanthanum tracer and freeze-fracture studies suggest that compartmentalisation of early bone matrix may be related to initial mineralisation. J Anat. 1992;181 (Pt 2)(345–56). [PubMed: 1295872]
48. Trumbore DC, Heideger WJ, and Beach KW. Electrical potential difference across bone membrane. Calcif Tissue Int. 1980;32(2):159–68. [PubMed: 6773633]
49. Barzel US. The skeleton as an ion exchange system: implications for the role of acid-base imbalance in the genesis of osteoporosis. J Bone Miner Res. 1995;10(10):1431–6. [PubMed: 8686497]
50. Borgens RB. Endogenous ionic currents traverse intact and damaged bone. Science. 1984;225(4661):478–82. [PubMed: 6740320]
51. Green J, and Kleeman CR. Role of bone in regulation of systemic acid-base balance. Kidney Int. 1991;39(1):9–26. [PubMed: 1706001]
52. Powell WF, Jr., Barry KJ, Tulum I, Kobayashi T, Harris SE, Bringhurst FR, and Pajevic PD. Targeted ablation of the PTH/PTHrP receptor in osteocytes impairs bone structure and homeostatic calcemic responses. J Endocrinol. 2011;209(1):21–32. [PubMed: 21220409]
53. Saini V, Marengi DA, Barry KJ, Fulzele KS, Heiden E, Liu X, Dedic C, Maeda A, Lotinun S, Baron R, et al. Parathyroid hormone (PTH)/PTH-related peptide type 1 receptor (PPR) signaling in osteocytes regulates anabolic and catabolic skeletal responses to PTH. J Biol Chem. 2013;288(28): 20122–34. [PubMed: 23729679]
54. Shin MM, Kim YH, Kim SN, Kim GS, and Baek JH. High extracellular Ca^{2+} alone stimulates osteoclast formation but inhibits in the presence of other osteoclastogenic factors. Exp Mol Med. 2003;35(3):167–74. [PubMed: 12858015]
55. Goltzman D, and Hendy GN. The calcium-sensing receptor in bone--mechanistic and therapeutic insights. Nat Rev Endocrinol. 2015;11(5):298–307. [PubMed: 25752283]
56. Cowin SC, and Cardoso L. Blood and interstitial flow in the hierarchical pore space architecture of bone tissue. J Biomech. 2015;48(5):842–54. [PubMed: 25666410]
57. Reid IR, Avenell A, Grey A, and Bolland MJ. Calcium Intake and Cardiovascular Disease Risk. Ann Intern Med. 2017;166(9):684–5.
58. Reid IR, Birstow SM, and Bolland MJ. Calcium and Cardiovascular Disease. Endocrinol Metab (Seoul). 2017;32(3):339–49. [PubMed: 28956363]
59. Reid B, Nuccitelli R, and Zhao M. Non-invasive measurement of bioelectric currents with a vibrating probe. Nat Protoc. 2007;2(3):661–9. [PubMed: 17406628]
60. Kunkel J, Cordeiro S, Xu Y, Shipley AM, and Feijo JA. The use of non-invasive ion-selective microelectrode techniques for the study of plant development In: Volkov AG ed. Plant Electrophysiology – Theory and Methods. Heidelberg: Springer-Verlag; 2006:109–37.
61. Kunkel JG, Nagel W, and Jercinovic MJ. Mineral fine structure of American lobster cuticle. J Shellfish Res. 2012;31(515–26).
62. Maeda A, Okazaki M, Baron DM, Dean T, Khatri A, Mahon M, Segawa H, Abou-Samra AB, Juppner H, Bloch KD, et al. Critical role of parathyroid hormone (PTH) receptor-1 phosphorylation in regulating acute responses to PTH. Proc Natl Acad Sci U S A. 2013;110(15): 5864–9. [PubMed: 23533279]
63. Rao CR Linear Statistical Inference and Its Applications. New York: John Wiley & Sons; 1965.
64. Parsons JA, Neer RM, and Potts JT, Jr., Initial fall of plasma calcium after intravenous injection of parathyroid hormone. Endocrinology. 1971;89(3):735–40. [PubMed: 5566389]
65. Dallas SL, Prideaux M, and Bonewald LF. The osteocyte: an endocrine cell … and more. Endocr Rev. 2013;34(5):658–90. [PubMed: 23612223]
66. Kalu DN, Hadji-Georgopoulos A, Sarr MG, Solomon BA, and Foster GV. The role of parathyroid hormone in the maintenance of plasma calcium levels in rats. Endocrinology. 1974;95(4):1156–65. [PubMed: 4416472]

67. Ramp WK, and McNeil RW. Selective stimulation of net calcium efflux from chick embryo tibiae by parathyroid hormone in vitro. Calcif Tissue Res. 1978;25(3):227–32. [PubMed: 709403]
68. Qing H, Ardeshirpour L, Pajevic PD, Dusevich V, Jahn K, Kato S, Wysolmerski J, and Bonewald LF. Demonstration of osteocytic perilacunar/canalicular remodeling in mice during lactation. J Bone Miner Res.27(5):1018–29.
69. Hirai T, Kobayashi T, Nishimori S, Karaplis AC, Goltzman D, and Kronenberg HM. Bone Is a Major Target of PTH/PTHrP Receptor Signaling in Regulation of Fetal Blood Calcium Homeostasis. Endocrinology. 2015;156(8):2774–80. [PubMed: 26052897]
70. Wysolmerski JJ. Osteocytes remove and replace perilacunar mineral during reproductive cycles. Bone. 2013;54(2):230–6. [PubMed: 23352996]
71. Teti A, and Zallone A. Do osteocytes contribute to bone mineral homeostasis? Osteocytic osteolysis revisited. Bone. 2009;44(1):11–6. [PubMed: 18977320]
72. Bonucci E Bone mineralization. Front Biosci (Landmark Ed). 2012;17(100–28). [PubMed: 22201735]
73. Wang W, Lewin E, and Olgaard K. Parathyroid hormone is not a key hormone in the rapid minute-to-minute regulation of plasma Ca2+ homeostasis in rats. Eur J Clin Invest. 1999;29(4):309–20. [PubMed: 10231343]
74. Lewin E, Wang W, and Olgaard K. Rapid recovery of plasma ionized calcium after acute induction of hypocalcaemia in parathyroidectomized and nephrectomized rats. Nephrol Dial Transplant. 1999;14(3):604–9. [PubMed: 10193806]
75. Loupy A, Ramakrishnan SK, Wootla B, Chambrey R, de la Faille R, Bourgeois S, Bruneval P, Mandet C, Christensen EI, Faure H, et al. PTH-independent regulation of blood calcium concentration by the calcium-sensing receptor. J Clin Invest. 2012;122(9):3355–67. [PubMed: 22886306]
76. Kantham L, Quinn SJ, Egbuna OI, Baxi K, Butters R, Pang JL, Pollak MR, Goltzman D, and Brown EM. The calcium-sensing receptor (CaSR) defends against hypercalcemia independently of its regulation of parathyroid hormone secretion. Am J Physiol Endocrinol Metab. 2009;297(4):E915–23. [PubMed: 19797241]
77. Huan J, Martuseviciene G, Olgaard K, and Lewin E. Calcium-sensing receptor and recovery from hypocalcaemia in thyroparathyroidectomized rats. Eur J Clin Invest. 2007;37(3):214–21. [PubMed: 17359489]
78. Talmage RV, Doppelt SH, and Fondren FB. An interpretation of acute changes in plasma 45Ca following parathyroid hormone administration to thyroparathyroidectomized rats. Calcif Tissue Res. 1976;22(2):117–28. [PubMed: 1000348]
79. Wongdee K, Riengrojpitak S, Krishnamra N, and Charoenphandhu N. Claudin expression in the bone-lining cells of female rats exposed to long-standing acidemia. Exp Mol Pathol. 2010;88(2): 305–10. [PubMed: 20035748]
80. Wongdee K, Pandaranandaka J, Teerapornpuntakit J, Tudpor K, Thongbunchoo J, Thongon N, Jantarajit W, Krishnamra N, and Charoenphandhu N. Osteoblasts express claudins and tight junction-associated proteins. Histochem Cell Biol. 2008;130(1):79–90. [PubMed: 18365232]

HIGHLIGHTS

1. PTH has no effect on rapid calcium flux at the bone/plasma interface
2. Osteocyte PTH receptor is not required for rapid calcium flux at this interface
3. Mice lacking osteocyte PTH receptor have fast calcemic response to PTH as controls
4. Bone mineral composition of PPR osteocyte KO mice differs from controls

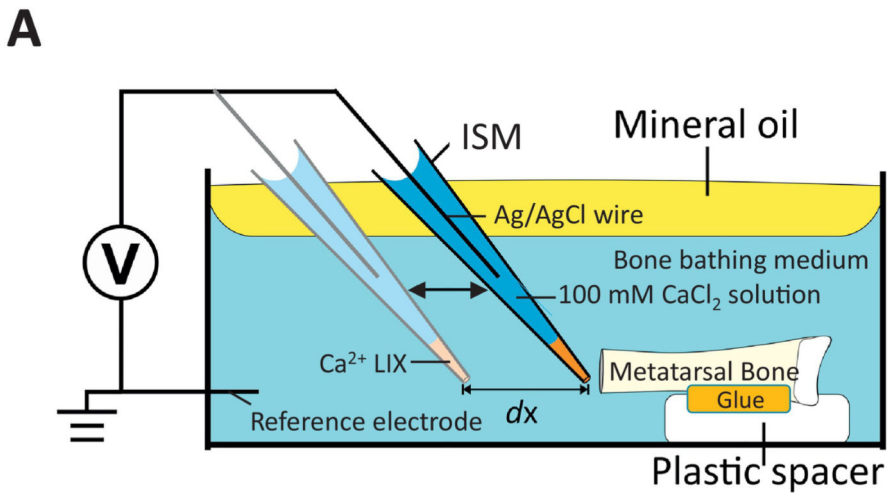

Figure 1:

A) Schematic representation of the experimental set-up. As shown in the diagram, the excised metatarsal bone is maintained in place by a drop of cyanoacrylate glue at the proximal epiphysis on a a plastic spacer fixed at the bottom of a standard 3.5-cm plastic Petri dish. The shaft was held parallel to the bottom of the dish to allow for ISM scanning of the exposed bone cortex of the distal extremity. The dish was filled with the appropriate pre-warmed (37°C) medium (5.4 ml) and positioned on the viewing stage. The ISM was immersed in the medium after which the medium surface was immediately covered with a thin layer of light, clear, pre-warmed (37°C) mineral oil. The oil layer greatly reduces temperature-driven convection flow and helps maintain pH by minimizing air exchange at the surface of the solution. The ISM is then stabilized at reference (light blue ISM, away from the bone) and then moved close to the bone surface (dark blue ISM).

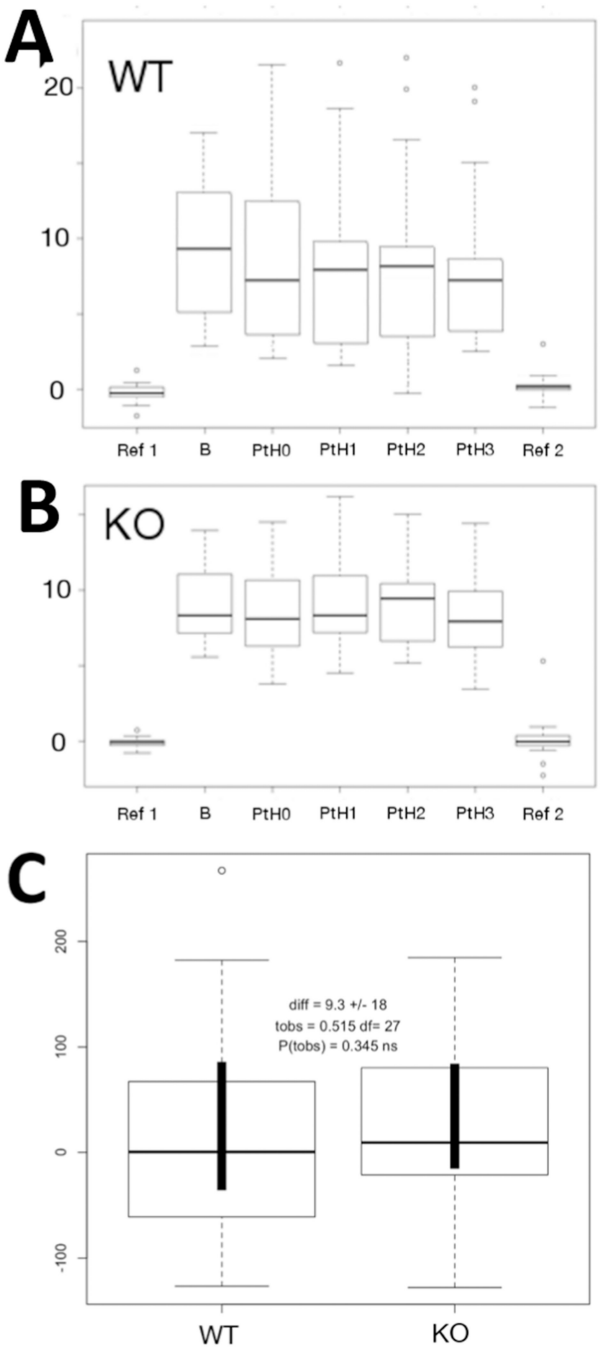

Figure 2:

Ca^{2+} fluxes in response to PTH. Acute PTH does not affect Ca^{2+} fluxes in metatarsal bones of Controls (A) or DMP1-PPRKO (B) animals. Comparison of Ca^{2+} slopes soon after adding PTH demonstrated no significant difference between PPRfl/fl controls (WT) and KO bones (C).

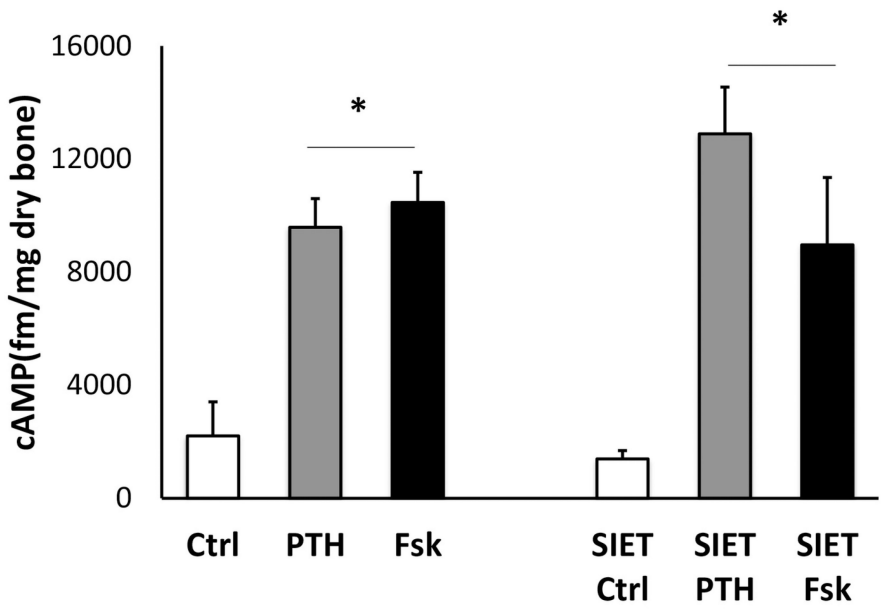

Figure 3:
cAMP responses to PTH and forskolin in metatarsal bones cultured in cAMP or SIET medium. Data is expressed as mean ± S.D.

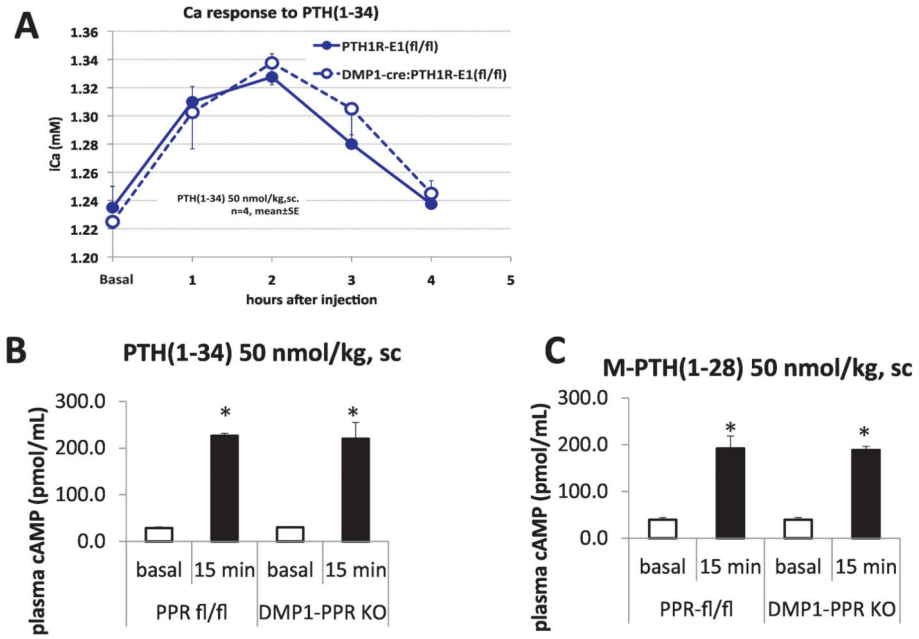

Figure 4:

In vivo acute calcemic responses to PTH in controls and DMP1-PPRfl/fl animals. 8–10 weeks old male mice (n=4 in each group) were injected with PTH or vehicle and Ca^{2+} analyzed after 1, 2, 3 and 4 hrs. Data is expressed as mean ± S.D.

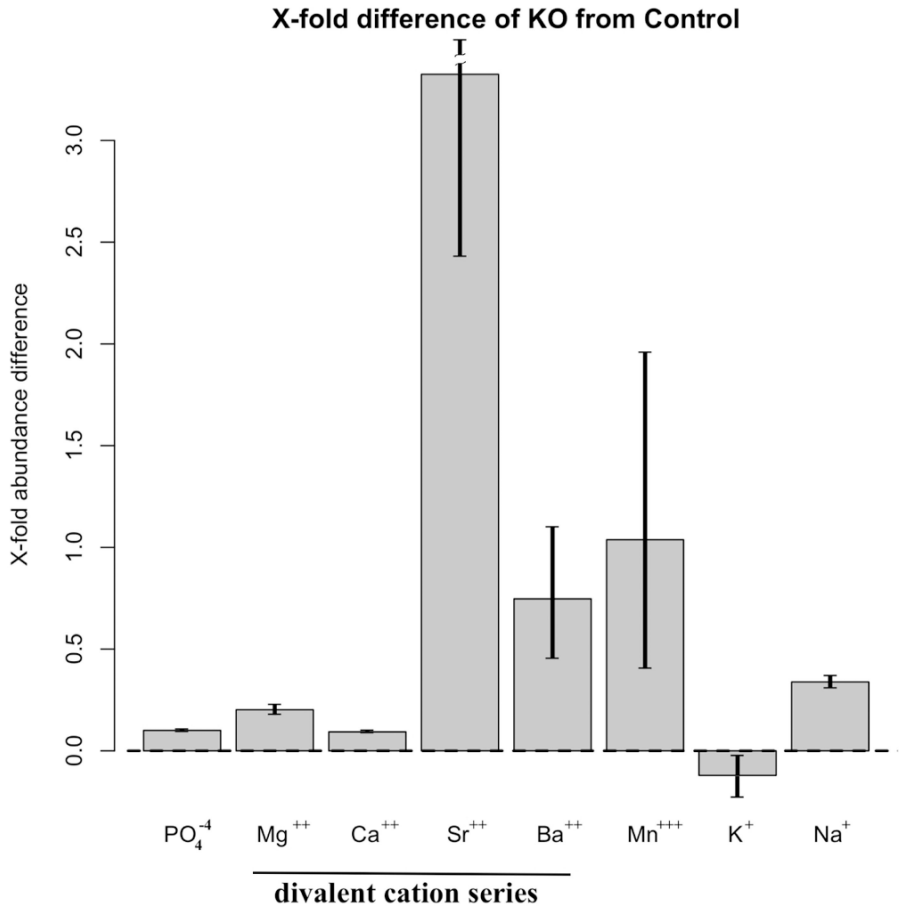

Figure 5:

Bone mineral composition in DMP1-PPRfl/fl bones. Fine mineral structure analysis of metatarsal bones from DMP1-PPRKO and control animals was performed with an Electron Microprobe. Data shown as fold changes in DMP1-PPRKO compared to littermate controls. Error bars are 95% CI (Confidence Intervals) of the mean. These data indicates that in the absence of PTH receptor signaling on osteocytes, there is a shift in the relative content of divalent cation and a relative accumulation of Sr^{2+}.